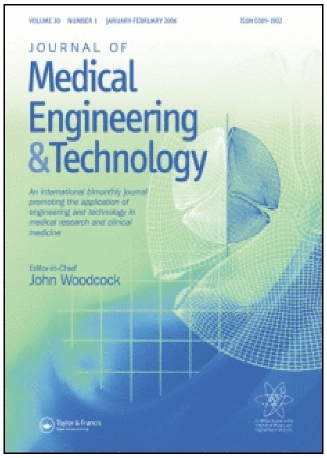
JOURNAL OF
Medical
Engineering
&Technology
Editor-in-Chief
John Woodcock

Journal of Medical Engineering & Technology, 2008, 1 – 12, i*First* article

Efficient FES triggering applying Kalman filter during sensory supported treadmill walking

I. CIKAJLO*†, Z. MATJAČIĆ† and T. BAJD‡

†Institute for Rehabilitation Republic of Slovenia, Linhartova 51, 1000 Ljubljana, Slovenia
‡Faculty of Electrical Engineering, University of Ljubljana, Tržaška 25, Ljubljana, Slovenia

In this paper an algorithm for a functional electrical stimulation (FES) gait re-education system for incomplete spinal cord injured persons, providing efficient stimulation triggering, is presented. During neurological impaired gait FES was provided as motor augmentation support. Simultaneously the gait kinematics were recorded using the proposed sensory system, which is equipped with a dual-axial accelerometer and a gyroscope. The sensory device was placed at the shank of the paretic leg. The data assessed were input into a mathematical algorithm applied for shank angle estimation. The algorithm is based on the Kalman filter, estimating the angle error and correcting the actual measurement. Furthermore the information was combined with other kinematic data for the purpose of efficient and reliable stimulation triggering. The algorithm was tested with preliminary measurements on several neurologically intact persons during even terrain and treadmill walking. Trial measurements were verified with a contactless optical measurement system, with FES only simulated on controller output. Later on a treadmill training in combination with FES triggering was carried out. The outcome of the measurements shows that the use of sensory integration may successfully solve the problem of data assessment in dynamic movement where an inclinometer does not provide sufficient information for efficient control of FES.

Keywords: Tilt sensor; Gait re-education; FES control; Rehabilitation engineering; Treadmill

1. Introduction

In the past most of our research has focused on restoration of functional movement after spinal cord injury (SCI). We have put a lot of effort into improving the role of functional electrical stimulation (FES) as an effective tool in gait restoration of incomplete SCI patients. We realized the necessity of FES gait training in the early period after spinal cord injury [1]. The candidates in [1] were all patients with upper motor neuron lesion, or in more clinical terms with thoracic or cervical lesion to the spinal cord. Only a few incomplete SCI patients were candidates for permanent FES. Most of them used FES only as a therapeutic device in the clinical environment or after being released from the rehabilitation centre. In these patients surface peroneal nerve stimulation was found to be useful for provoking flexion response resulting in the swing phase of walking. The most commonly used method for FES triggering has been application of the heel switch, where the strain gauge or FSR based switch is placed into the shoe and starts the stimulation after the user's heel leaves the ground. The precise instant of triggering is set individually for every patient using a time delay. The heel switch application is not the most appropriate method, because it forces the patient to be booted while using the stimulator. In spite of this disadvantage it was well accepted by our patients especially when applied to crutch users. In therapeutic FES gait training as well as in hemiplegic patients the hand push-button triggering was applied successfully [2]. Several existing systems employing peroneal nerve stimulation have

*Corresponding author. Email: imre.cikajlo@mail.ir-rs.si

Journal of Medical Engineering & Technology
ISSN 0309-1902 print/ISSN 1464-522X online © 2008 Informa UK Ltd.
http://www.tandf.co.uk/journals
DOI: 10.1080/03091900601029627

applied sensory information to trigger FES automatically during walking. The sensory information could be provided by use of simple artificial sensors [3]. Data collected by a pair of miniature accelerometers were used to distinguish between the stance and swing phase. Automatic detection algorithms were used to identify the appropriate phase of walking and to control the FES. Dai *et al*. [4] applied various tilt sensors to assess data appropriate for estimation of human body inclination, i.e. the information that served for prediction of the patient's intention of walking progress. The threshold-saturation algorithm was then applied.

In recent years a great deal of research has been carried out into therapeutical FES combined with treadmill rehabilitation. It has been shown that repeatable action significantly improves any functional movement if the possibility of central nervous system (CNS) reorganization exists [5]. Therefore the FES rehabilitative system for re-education of walking [6] aimed not only to deliver electrical stimulation to the paralysed muscles, but also to assess the sensory information from the paralysed limb and provide this information to the patient; providing part of the processed information to the stimulator control unit [7] was suggested. The FES rehabilitation systems for re-education of walking are intended to be used for incomplete SCI persons soon after the accident or onset of disease. These systems are to be used within rehabilitation centres and applied by therapists. Surface electrical stimulation is therefore appropriate.

So far we have tried manual FES triggering using a push-button [8] but it was realized that the physiotherapist was unable to keep up with the patient's walking speed during treadmill training and consequently triggered the FES earlier or later than required. Therefore we were not able to assure the required repeatability of treadmill walking. To avoid the problem a goniometer was placed in knee joint, measuring the knee angle. The information was used to automatically trigger the FES. The important fact was that triggering had to occur before the swing phase took place. To avoid malfunctioning during the stance phase the knee angle information was integrated with swing phase detection [9]. However the problem of goniometer slipping has appeared and patients have complained of inconvenience. Therefore instead of the goniometer an application of already used sensors for swing phase detection and estimation was considered. Hereby the efficient algorithm that provided applicable information for FES triggering was a good and helpful tool in overcoming the described problems and has proven effective when additional sensors could not be set due to the patient's inconvenience.

The algorithm for shank angle estimation was developed from the widespread idea of orientation estimation with gyroscopes or inclinometers [4,10]. The main idea however was to develop a successful and applicable algorithm that will be able to take advantage of the applied sensory device in order to replace the unreliable goniometer in FES triggering. In this paper we present the application of such an approach during treadmill walking.

Preliminary measurements were aimed at testing the reliability of the approach in the clinical environment. But before the clinical trial and application in the existing gait re-education system [7], a test of kinematic accordance with an optical measurement system was performed. The optical motion analysis system Vicon 370 (© Vicon Motion Systems, Oxford, UK), which is capable of kinematic data analysis, was used as the reference. The outcomes gave us inspiration for further work. We are looking forward to developing a clinically applicable approach.

2. Methods

2.1. Hardware description

In this research a sensory system, developed from a previous experimental aluminium plate mounted sensory system [11], was used. A new modular approach is based on microcontroller (Atmel AT90S4434, Atmel Corporation, San Jose, CA, USA) supervised data acquisition. Two-axis accelerometer (Analog Devices ADXL210E, Norwood, MA, USA) with digitally filtered output was used. The bandwidth was set from 0 to 50 Hz. The digital outputs of both axes were assessed by digital inputs of the micro-controller. A single-axial gyroscope (Murata ENC 03JA, Murata Manufacturing Co., Ltd., Nagaokakya-shi, Kyoto, Japan) was added to assess the angular velocity when the device is attached to the moving object. The gyroscope's analogue output was amplified and filtered with an analogue low-pass filter with a cut-off frequency of 126 Hz and afterwards sampled by a microcontroller internal A/D converter (10 bits, up to 15 kHz). All acquired data were transmitted via RS232 communication port to a personal computer (PC), where further mathematical and control algorithms were performed. The sensory device (figure 1) was attached to the front side of the patient's shank by Velcro straps.

The existing sensory device, consisting of two major types of sensor for orientation estimation, would be a good solution or substitution for the goniometer or heel switch. The dynamic characteristics of walking, especially heel strike, discouraged us from using an accelerometer based inclinometer as the only source of information. Therefore we considered the use of integrated gyroscope signal as the principal source of information to estimate the shank inclination. Gyroscope is liable to bias due to temperature change, random walk and noise [12], so an efficient mathematical approach like the Kalman filter [13] was considered a suitable solution. The Kalman filter implements measured data to correct the estimated model output. In this paper the Kalman filter is used to correct the estimated shank angle using a gyroscope state-space model.

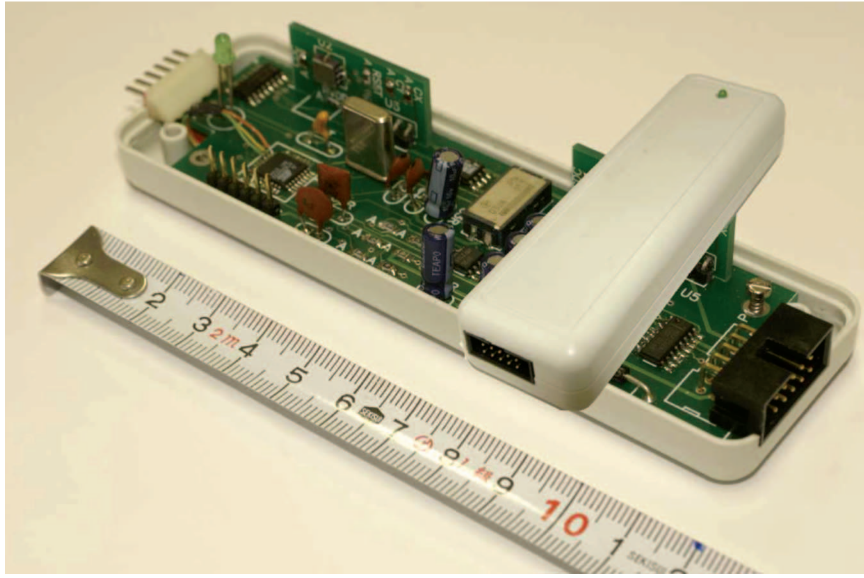

Figure 1. Multisensory device consists of two-axial accelerometer, single-axial gyroscope and microcontroller.

2.2. *Kalman filter (estimator) theory*

The discrete Kalman filter (estimator) is based on the additional external measurement source used for the estimated system state-space variable correction and may be represented by the following equation:

$$\hat{\boldsymbol{x}}_k = \hat{\boldsymbol{x}}_k^- + \boldsymbol{K}_{\mathbf{Kal}}(z_k - \boldsymbol{H}_k\hat{\boldsymbol{x}}_k^-), \tag{1}$$

where $\boldsymbol{K}_{\mathbf{Kal}}$ is a Kalman gain, $\hat{x}_k$ the estimated state and $\boldsymbol{H}_k$ the output matrix of the implemented system model and z_k the external measurement source.

The implemented system model with belonging input noise $\boldsymbol{w}_k$ and output noise $\boldsymbol{v}_k$ may be described by the discrete state-space model [14]:

$$\begin{aligned} \boldsymbol{x}_{k+1} &= \phi_k\boldsymbol{x}_k + \boldsymbol{B}_k\boldsymbol{u}_k + \boldsymbol{w}_k \\ \boldsymbol{y}_k &= \boldsymbol{H}_k\boldsymbol{x}_k + \boldsymbol{v}_k, \end{aligned} \tag{2}$$

where the output of the system model is presented by $\boldsymbol{y}_k$, the state-space matrix by ϕ_k, input matrix by $\boldsymbol{B}_k$, system input by $\boldsymbol{u}_k$ and output matrix by $\boldsymbol{H}_k$. We may also suppose that both system noises could be presented with white noise with covariance matrices $\boldsymbol{Q}_{wk}$ and $\boldsymbol{R}_{vk}$:

$$E\left[\boldsymbol{w}_k\boldsymbol{w}_i^T\right] = \begin{cases} \boldsymbol{Q}_{w_k} & : i = k \\ 0 & : i \neq k \end{cases} \tag{3}$$

$$E\left[\boldsymbol{v}_k\boldsymbol{v}_i^T\right] = \begin{cases} \boldsymbol{R}_{v_k} & : i = k \\ 0 & : i \neq k \end{cases} \tag{4}$$

$$E\left[\boldsymbol{w}_k\boldsymbol{v}_i^T\right] = \{ 0 \quad : \forall k \wedge \forall i. \tag{5}$$

The calculation of the Kalman gain $\boldsymbol{K}_{\mathbf{Kal}}$ rely on minimization of the error covariance matrix $\boldsymbol{P}_k$. In order to calculate the matrix we define the estimation error:

$$e_k^- = \hat{\boldsymbol{x}}_k - \hat{\boldsymbol{x}}_k^-, \tag{6}$$

where $\hat{\boldsymbol{x}}_k^-$ is an a priori estimation from system model and $\hat{\boldsymbol{x}}_k$ the Kalman filter state estimation. From here on we may define the error covariance matrix $\boldsymbol{P}_k$:

$$\boldsymbol{P}_k^- = \boldsymbol{E}\left[e_k^- e_k^{-\boldsymbol{T}}\right] = \boldsymbol{E}\left[(\hat{\boldsymbol{x}}_k - \hat{\boldsymbol{x}}_k^-)(\hat{\boldsymbol{x}}_k - \hat{\boldsymbol{x}}_k^-)^{\boldsymbol{T}}\right] \tag{7}$$

and substitute the Kalman filter state estimation with equation (1). We get the following equation:

$$\boldsymbol{P}_k = (\boldsymbol{I} - \boldsymbol{K}_{\mathbf{Kal}}\boldsymbol{H}_k)\boldsymbol{P}_k^-(\boldsymbol{I} - \boldsymbol{K}_{\mathbf{Kal}}\boldsymbol{H}_k)^{\boldsymbol{T}} + \boldsymbol{K}_{\mathbf{Kal}}\boldsymbol{R}_{vk}\boldsymbol{K}_{\mathbf{Kal}}^{\boldsymbol{T}}. \tag{8}$$

From calculating the derivative of equation (8), on $\boldsymbol{K}_{\mathbf{Kal}}$ and making it equal to 0 we can express the Kalman filter gain $\boldsymbol{K}_{\mathbf{Kal}}$:

$$\boldsymbol{K}_{\mathbf{Kal}} = \boldsymbol{P}_k^-\boldsymbol{H}_k^{\boldsymbol{T}}(\boldsymbol{H}_k\boldsymbol{P}_k{}^-\boldsymbol{H}_k^{\boldsymbol{T}} + \boldsymbol{R}_{vk})^{-1}. \tag{9}$$

Since the Kalman filter (estimator) algorithm is recursive it is suitable for numerical operations. We may present it as a loop algorithm that needs initial conditions $\hat{x}(0)^-$ and $\boldsymbol{P}_0^-$ to begin the calculation process. From initial conditions $\boldsymbol{K}_{\mathbf{Kal}}$ (equation (9)) is determined. In subsequent steps, the estimated state is corrected by the measured signal z_k in equation (1). The corrected state of the system $\hat{\boldsymbol{x}}_k$ is now considered as an applicable filter output.

The recursive calculation continues with a calculation of the recursive error covariance matrix $\boldsymbol{P}_k$:

$$\boldsymbol{P}_k = (\boldsymbol{I} - \boldsymbol{K}_{\mathbf{Kal}}\boldsymbol{H}_k)\boldsymbol{P}_k^-. \tag{10}$$

After the present states $\hat{\boldsymbol{x}}_k$ (the filter output) and appertaining covariance matrix $\boldsymbol{P}_k$ are determined, the state of the system for the next step can be estimated:

$$\begin{aligned}\hat{\boldsymbol{x}}_{k+1}^{-} &= \phi_k \hat{\boldsymbol{x}}_k + \boldsymbol{B}\boldsymbol{u}_k \\ \boldsymbol{P}_{k+1}^{-} &= \phi_k \boldsymbol{P}_k \phi_k^{\boldsymbol{T}} + \boldsymbol{Q}_{\boldsymbol{wk}}.\end{aligned} \tag{11}$$

After equation (11) the recursive algorithm is repeated from renewed Kalman gain $\boldsymbol{K}_{\mathbf{Kal}}$ (equation (9)) and corrected filter output (equation (1)).

2.3. Shank angle estimation

Treadmill walking mainly consists of movement in the sagittal plane and less in the lateral plane. In our case we may simplify the shank movement during swing phase to sagittal plane movement only. While the applied sensory device is attached in front of the shank (figure 2), the data assessed are in the moving direction. Therefore a simplified shank angle estimation may be used.

The gyroscope behavior may be modelled considering the actual angular velocity, undesired bias that causes a cumulative error during signal integration, sensor noise and integration noise [12]:

$$\begin{aligned}\dot{\theta} &= \omega + b + n_r \\ \dot{b} &= n_w\end{aligned} \tag{12}$$

The above equation is presented in state-space for further analysis:

$$\begin{bmatrix}\dot{\theta} \\ \dot{b}\end{bmatrix} = \begin{bmatrix}0 & 1 \\ 0 & 0\end{bmatrix}\begin{bmatrix}\theta \\ b\end{bmatrix} + \begin{bmatrix}\omega \\ 0\end{bmatrix} + \begin{bmatrix}n_r \\ n_\omega\end{bmatrix}, \tag{13}$$

where the angular velocity is presented by ω, bias by b and uncorrelated Gauss noises:

$$\begin{aligned}&E[\boldsymbol{n}_r] = 0 \\ &E[\boldsymbol{n}_r \boldsymbol{n}_r'] = N_r \delta(t - t') \\ &E[\boldsymbol{n}_\omega] = 0 \\ &E[\boldsymbol{n}_\omega \boldsymbol{n}_\omega'] = N_w \delta(t - t').\end{aligned} \tag{14}$$

The noise N_r is caused by gyroscope sensor, while the integration noise N_ω is a consequence of transfer function $\frac{1}{s}$ filtering. All noise values are estimated or taken from the sensor manual.

According to figure 3 the Kalman filter estimates the shank angle error while correcting the estimated value with external measurement $\Delta\theta_m$. The accelerometer based inclinometer is not suffering from bias, which is the main source of gyroscope based angle estimation error. For successful implementation of the proposed method a differential angle error model is needed. Before proposing the differential model the following relations should be considered:

$$\begin{aligned}\Delta\hat{\theta} &= \theta - \hat{\theta} \\ \Delta\theta_m &= \theta - \theta_m,\end{aligned} \tag{15}$$

where θ is the integrated gyroscope value and θ_m is the bias-free inclination estimated by accelerometer (a part of the sensory device) based inclinometer:

$$\theta_m = \left[\frac{\pi}{2} - \arctan\frac{a_{t0}}{a_{r0}}\right]. \tag{16}$$

The shank angle error model due to the scheme (figure 3) and suitable for Kalman filter/estimator may be written in the state-space form:

$$\begin{bmatrix}\Delta\dot{\hat{\theta}} \\ \Delta\dot{\hat{b}}\end{bmatrix} = \begin{bmatrix}0 & 1 \\ 0 & 0\end{bmatrix}\begin{bmatrix}\Delta\hat{\theta} \\ \Delta\hat{b}\end{bmatrix} + \begin{bmatrix}n_r \\ n_w\end{bmatrix}. \tag{17}$$

Furthermore, the error model output, the estimated shank angle error, is defined as:

$$\Delta z = \begin{bmatrix}1 & 0\end{bmatrix}\begin{bmatrix}\Delta\hat{\theta} \\ \Delta\hat{b}\end{bmatrix} + n_\theta, \tag{18}$$

where n_θ presents the measurement noise caused by accelerometer based inclinometer.

After the shank angle error estimation model had been pulled off it was implemented into the Kalman filter:

$$\phi = \begin{bmatrix}0 & 1 \\ 0 & 0\end{bmatrix} \quad \boldsymbol{H} = \begin{bmatrix}1 & 0\end{bmatrix} \quad \boldsymbol{B} = 0, \tag{19}$$

or in state-space form:

$$\begin{aligned}\Delta\dot{\boldsymbol{x}} &= \phi\Delta\boldsymbol{x} + \boldsymbol{n} \\ \Delta z &= \mathbf{H}\Delta\boldsymbol{x} + \boldsymbol{n}_\theta.\end{aligned} \tag{20}$$

Measurement noise R_v and system noise Q_w matrix needed for the Riccati equation can be expressed in the following form:

$$\begin{aligned}Q_w &= \begin{bmatrix}N_r & 0 \\ 0 & N_w\end{bmatrix} \\ R_v &= N_\theta.\end{aligned} \tag{21}$$

From the equation for continuous Kalman filter [15]:

$$\dot{\boldsymbol{P}} = \phi\boldsymbol{P} + \boldsymbol{P}\phi^{\boldsymbol{T}} + Qw - \boldsymbol{P} - \boldsymbol{P}\boldsymbol{H}^{\boldsymbol{T}} R_v^{-1} \boldsymbol{H}\boldsymbol{P} \tag{22}$$

we may derive the analytical Kalman gain by using equation (9):

$$\boldsymbol{K}_{\mathbf{Kal}} = \begin{bmatrix}\sqrt{\frac{N_r + 2\sqrt{N_\omega N_\theta}}{N_\theta}} \\ \sqrt{\frac{N_\omega}{N_\theta}}\end{bmatrix} = \begin{bmatrix}k_1 \\ k_2\end{bmatrix}. \tag{23}$$

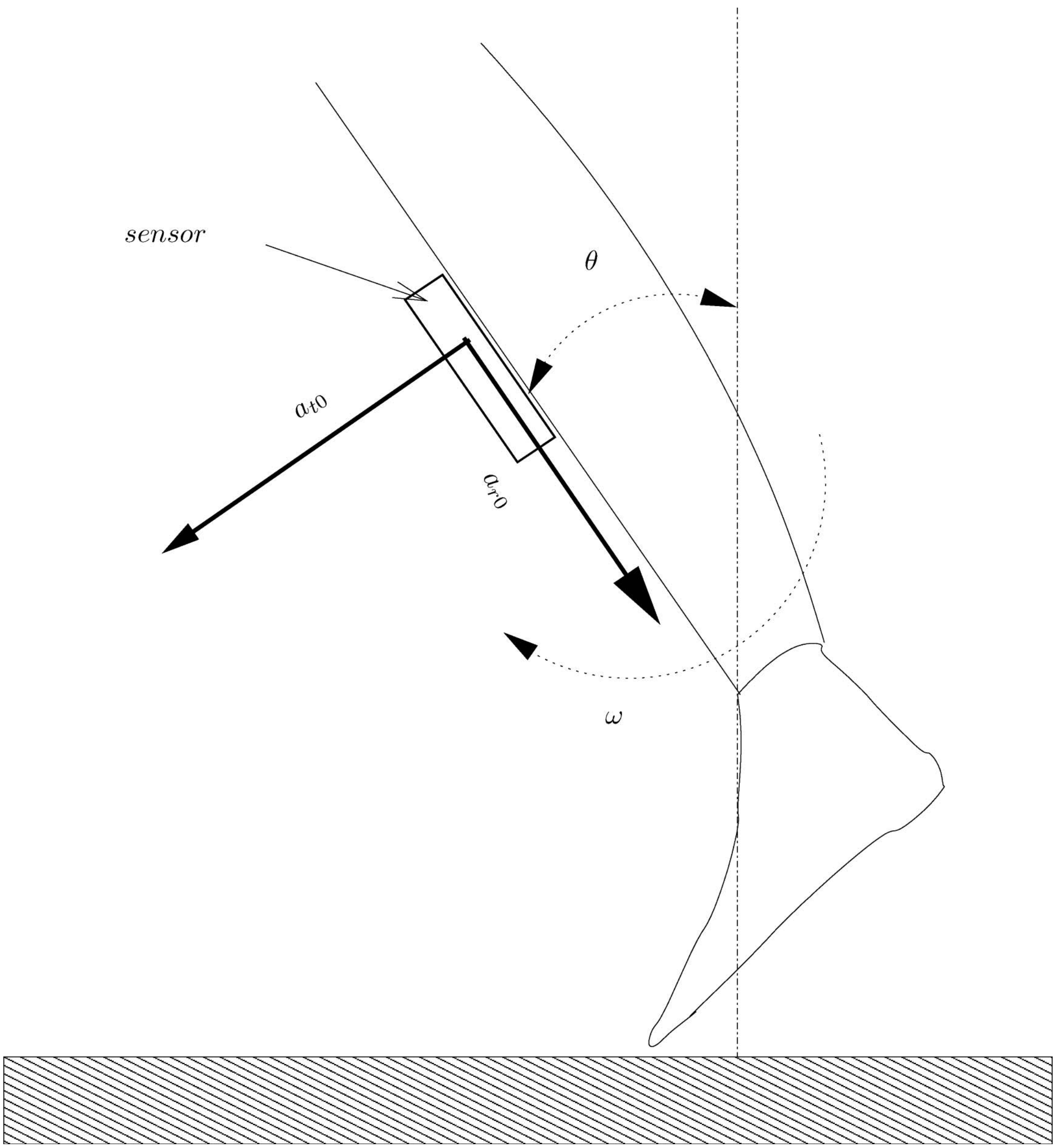

Figure 2. Lower extremity in swing phase. The sensory system is attached to the shank. The tangential a_{t0} and radial a_{r0} acceleration assessed by two-axis accelerometer and the shank angular velocity ω are presented.

Therefore the Kalman filter equation (following figure 3 and equations (1) and (15)) for shank angle error estimation would be as follows:

$$\begin{bmatrix} \Delta\dot{\hat{\theta}} \\ \Delta\dot{\hat{b}} \end{bmatrix} = \frac{d}{dt}\begin{bmatrix} \Delta\hat{\theta} \\ \Delta\hat{b} \end{bmatrix} = \begin{bmatrix} 0 & 1 \\ 0 & 0 \end{bmatrix}\begin{bmatrix} \Delta\hat{\theta} \\ \Delta\hat{b} \end{bmatrix} + \begin{bmatrix} k_1 \\ k_2 \end{bmatrix}(\Delta\theta_m - \Delta\hat{\theta}), \tag{24}$$

where k_1 and k_2 present the Kalman gain. While the shank angle estimation was performed only for planar motion, the Kalman filter became linear and the Kalman gain remained constant.

Considering equation (15) and the constant Kalman gain we may expand the equation and describe the system in figure 3 in the state-space formulation:

$$\frac{d}{dt}\begin{bmatrix} \theta - \hat{\theta} \\ b - \hat{b} \end{bmatrix} = \begin{bmatrix} 0 & 1 \\ 0 & 0 \end{bmatrix}\begin{bmatrix} \theta - \hat{\theta} \\ b - \hat{b} \end{bmatrix} + \begin{bmatrix} k_1 \\ k_2 \end{bmatrix}(\theta - \theta_m - (\theta - \hat{\theta})) \tag{25}$$

Replacement of the $\dot{\theta} - b$:

$$\omega = \dot{\theta} - b \tag{26}$$

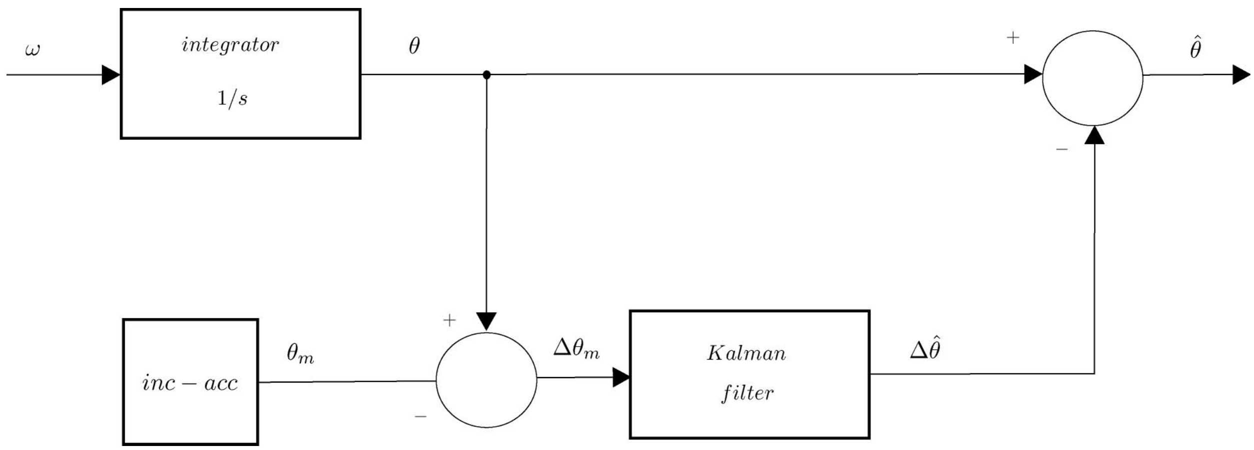

Figure 3. System for shank angle estimation. The Kalman filter is estimating the shank angle error while using the accelerometer based inclinometer (inc–acc) measurement.

leads us to the final state-space equation of the complete scheme in figure 3, where θ_m, ω are inputs and $\hat{\theta}$ presents the desired output; it is suitable for numerical operations:

$$\frac{d}{dt}\begin{bmatrix}\hat{\theta}\\ \hat{b}\end{bmatrix} = \begin{bmatrix}0 & 1\\ 0 & 0\end{bmatrix}\begin{bmatrix}\hat{\theta}\\ \hat{b}\end{bmatrix} + \begin{bmatrix}1\\ 0\end{bmatrix}\omega + \begin{bmatrix}k_1\\ k_2\end{bmatrix}(\theta_m - \hat{\theta}) \qquad (27)$$

2.4. Filter analysis in the frequency domain

The shank ankle estimation equation (27) is based on scheme (figure 3). For further frequency domain analysis we applied Laplace transform to the equation:

$$s\begin{bmatrix}\hat{\Theta}(s)\\ \hat{B}(s)\end{bmatrix} = \begin{bmatrix}0 & 1\\ 0 & 0\end{bmatrix}\begin{bmatrix}\hat{\Theta}(s)\\ \hat{B}(s)\end{bmatrix} + \begin{bmatrix}1\\ 0\end{bmatrix}\Omega(s) + \begin{bmatrix}k_1\\ k_2\end{bmatrix}(\Theta_m(s) - \hat{\Theta}(s)) \qquad (28)$$

and expressed the desired output, estimated shank angle $\hat{\Theta}$:

$$\begin{aligned}\hat{\Theta}(s) &= \frac{s^2}{s^2 + k_1 s + k_2}\cdot\frac{\Theta(s)}{s} + \frac{k_1 s + k_2}{s^2 + k_1 s + k_2}\cdot\Theta_m(s)\\ &= G(s)\frac{\Theta(s)}{s} + (1 - G(s))\Theta_m(s)\end{aligned} \qquad (29)$$

The summands of equation (29) may be presented as two complementary *2nd* order filters, $G(s)$ and $1 - G(s)$. The function $G(s)$ filters the integrated signal of the gyroscope and its behaviour is comparable to a high-pass filter. Conversely, the summand $1 - G(s)$ may represent the low-pass filter. The frequency analysis shows an another possible approach, designing two complementary filters. Usually the approach is based on neural networks learning or trial-error algorithm determining the appropriate filter coefficients [16].

A bode plot (figure 4) of both summands in equation (29) presents the frequency characteristics of both complementary filters that was equal to the characteristics of the proposed scheme in figure 3. The cut-off frequency was 2.27 Hz.

3. Results

3.1. Verification of the approach with camera based system

The preliminary measurements were carried out to determine whether the shank angle estimation algorithm would satisfy the demand for accurate measurements needed to control the FES and to provide reliable information on the quality of each accomplished swing of the extremity. We were looking for significant peaks in the assessed signals that we had been able to use for the purpose of triggering of the electrical stimulation. Therefore we used the optical motion analysis system Vicon (©Vicon Motion Systems) to confirm the approach that has replaced the use of goniometers in the gait re-education system [7]. Two healthy subjects AO (male, 172 cm, 65 kg, 24 years) and IC (male, 173 cm, 74 kg, 29 years) participated in the preliminary test. Their task was to walk with normal and slow pace, comparable with walking speed of the incomplete SCI patient(0.7–1.2 km h^{-1}) [7].

The upper graph of figure 5 presents the time-course of the shank during walking. These measurements were supported by the Vicon Motion System and a comparison between the assessed data and the data proposed by the described filtering algorithm was carried out simultaneously. The shank angle was determined from pelvis, hip and knee joint angles:

$$\theta_{shank} = \vartheta_{hip} - \vartheta_{pelvis} - \vartheta_{knee}. \qquad (30)$$

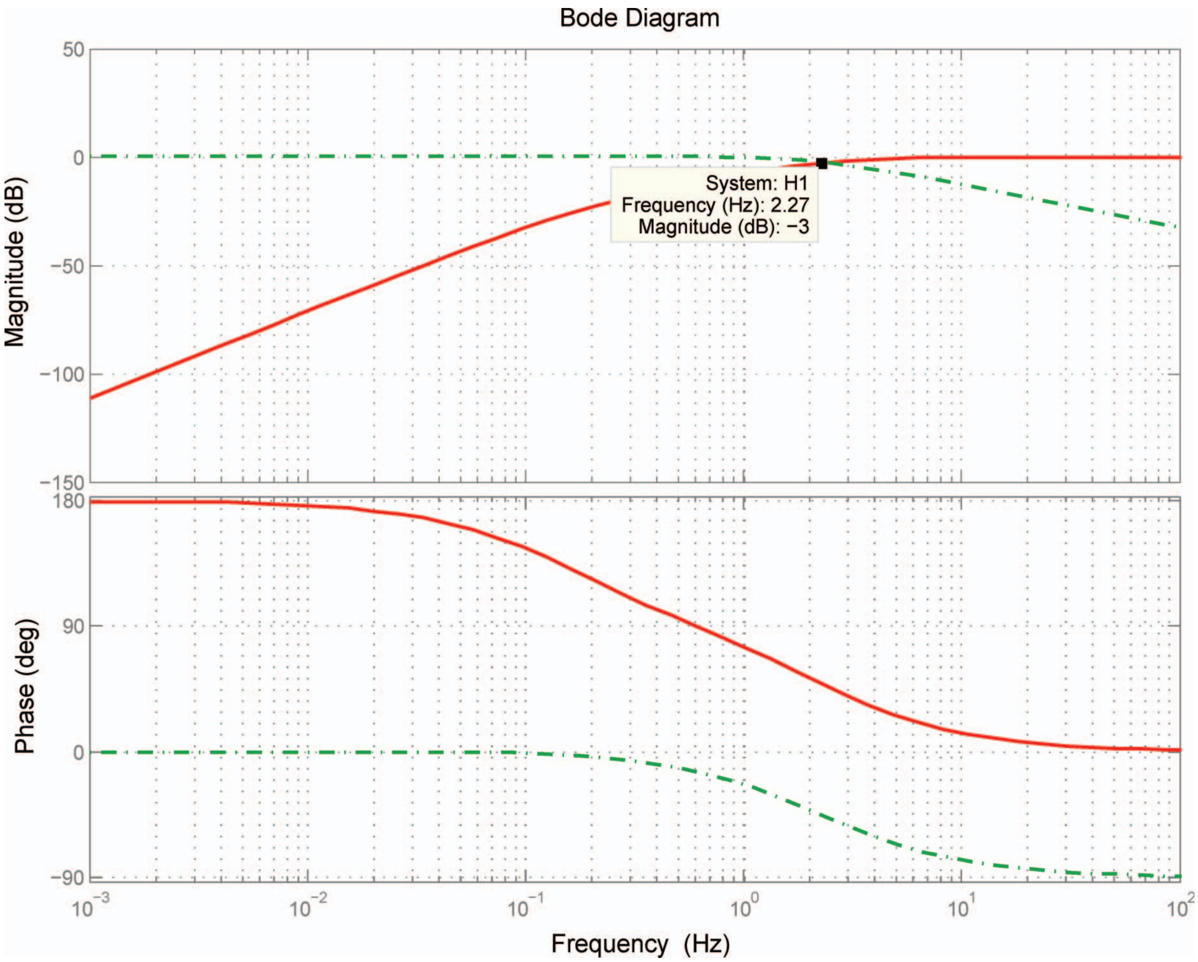

Figure 4. Bode diagram after Laplace analysis of the proposed solution for shank angle. Two summands are presented as two separate (but complementary) filter characteristics.

Figure 6 demonstrates the advantage of sensory integration. The implementation of the Kalman filter could in this case overcome the inconvenience caused by single sensor use. The shank ankle, determined by two-axial accelerometer, contains high frequencies, caused by heel strike, while the gyroscope is well known for its bias, most likely as a consequence of temperature change. The integration of the gyroscope bias resulted in a ramp response.

To evaluate the fitting and reliability of the proposed approach we calculated the cross-correlation coefficient between the data assessed by the Vicon Motion System and the Kalman filter sensor output for $N = 75$ gait cycles [17] using:

$$\rho_{\theta_{shank},\hat{\theta}}(t,\tau) = \frac{E[(\theta_{shank}(t) - m_m(t)) \cdot (\hat{\theta}(t+\tau) - m_r(t+\tau))]}{\sqrt{E[(\theta_{shank}(t) - m_m(t))^2 \cdot (\hat{\theta}(t+\tau) - m_r(t+\tau))^2]}}, \tag{31}$$

where m represents the mean of the signal, N is a number of samples included into computation and τ means a time delay, while $E[\theta_{shank}(t) \cdot \hat{\theta}(t+\tau)]$ is expressed:

$$E[\theta_{shank}(t) \cdot \hat{\theta}(t+\tau)] = \frac{1}{N}\sum_{k=1}^{N} \theta_{shank}(t) \cdot \hat{\theta}(t+\tau) \tag{32}$$

In equation (32) θ_{shank} the shank angle was computed from Vicon data, while $\hat{\theta}$ presents the data output of the indirect Kalman filter based approach. When the calculated coefficient $\rho_{\theta_{shank},\hat{\theta}}$ was close to 0, there was no correlation between the signals and as this approached 1, more signal resemblance was expected.

The correlation coefficient varied from 0.949 to 0.962 in several gait cycles. Unfortunately we have not been able to assess all the gait cycles from single walking time-course due to the Vicon motion assessment constraints; therefore we used data from several measurements of the same person and performed a correlation between data

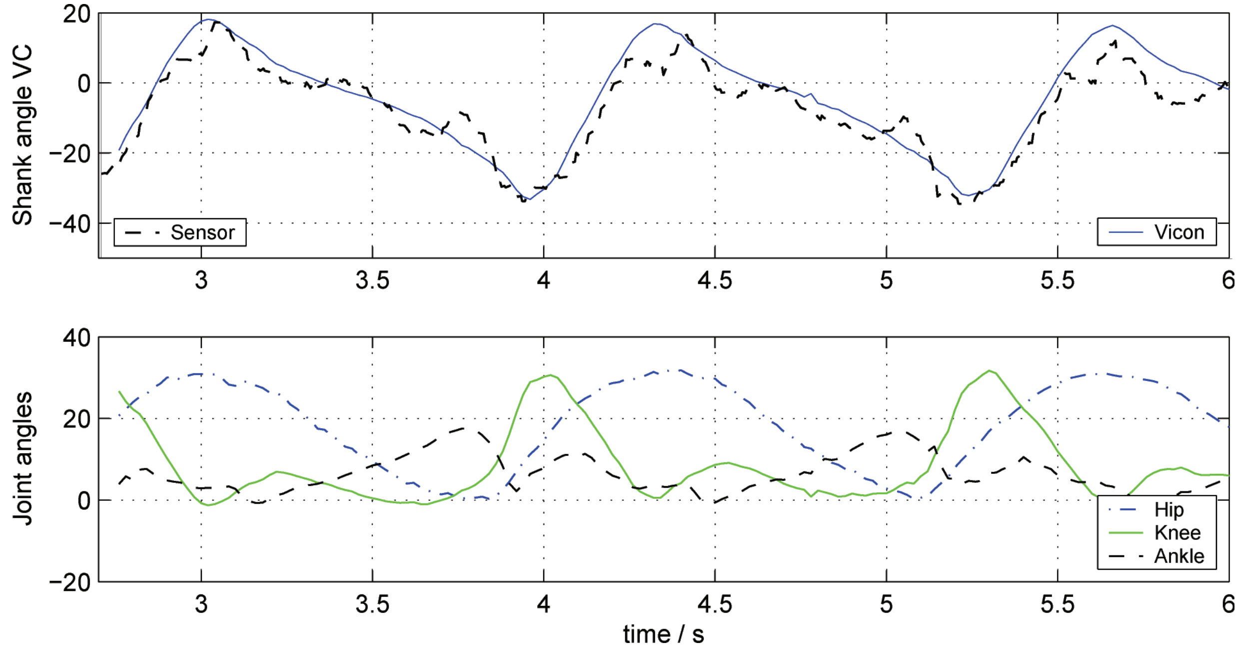

Figure 5. Kinematic analysis of the subject's IC even terrain walking. The comparison of the algorithm outcomes (sensor) and Vicon Motion Analysis System is shown. On the graph below joint angles calculated from Vicon data are also shown.

estimated by the Kalman filter versus Vicon in each single gait cycle. Afterwards we calculated the mean and the standard deviation (σ) to express the compliance of both signals:

$$\begin{aligned}\overline{\rho}_{\theta_{shank},\hat{\theta}} &= \frac{1}{N}\sum \rho_i \pm 2\sigma \\ &= 0.955 \pm 0.009.\end{aligned} \tag{33}$$

We realized that the compliance was almost perfect, as shown by $\rho = 0.955$, and the deviation between gait cycles was very low ($\sigma = 0.009$). There was no drifting of the estimated angle as in the integrated gyroscope signal. However, during initial foot contact and in stance phase we noticed deviations. Those deviations appear to be a contribution of the accelerometer signals. On the other hand it was obvious that the Vicon shank angle measurements were repeatable and reliable (figure 6). We did not pay attention to dynamic disturbances during stance phase, as the emphasis in our application is on swing phase. Parenthetically we have to take into consideration also that the placement of the device on the right shank might not have been perfect and might have slipped on occasion. In this case we also presume that the Vicon outcomes were absolutely accurate, although there might have been a slight marker displacement.

3.2. Algorithm application in the field of FES

The purpose of the algorithm is to trigger functional electrical stimulation. Following our experience and general knowledge of gait analysis [17] we have determined the start of the swing phase. The patients that use peroneal nerve stimulation to invoke the flexion reflex [1] need motor augmentation in the midswing phase when the lower extremity proceeds into the forward swing. Thus the stimulation could be triggered when the shank angle reaches 20° inclination. As shown in figure 5 the related event occurred before the peak in shank angle time-course. The stimulation trigger was determined using threshold algorithm in conjunction with the detected swing phase [9] and shank angular velocity. The latter prevented any triggering during the swing phase and uniformly defined the triggering instant of the electrical stimulation. After the swing phase was brought to an end and the initial contact took place, the stimulation was stopped. Due to the clinical demands and patient's needs as well as physiotherapist's wishes the instant of triggering should have an option to be delayed for the pre-set time constant. Comparison of the both graphs in figure 7 gives us the complete picture of the shank angle estimation use in the gait re-education system.

As the proposed algorithm was intended for the gait re-education system we have also performed a few

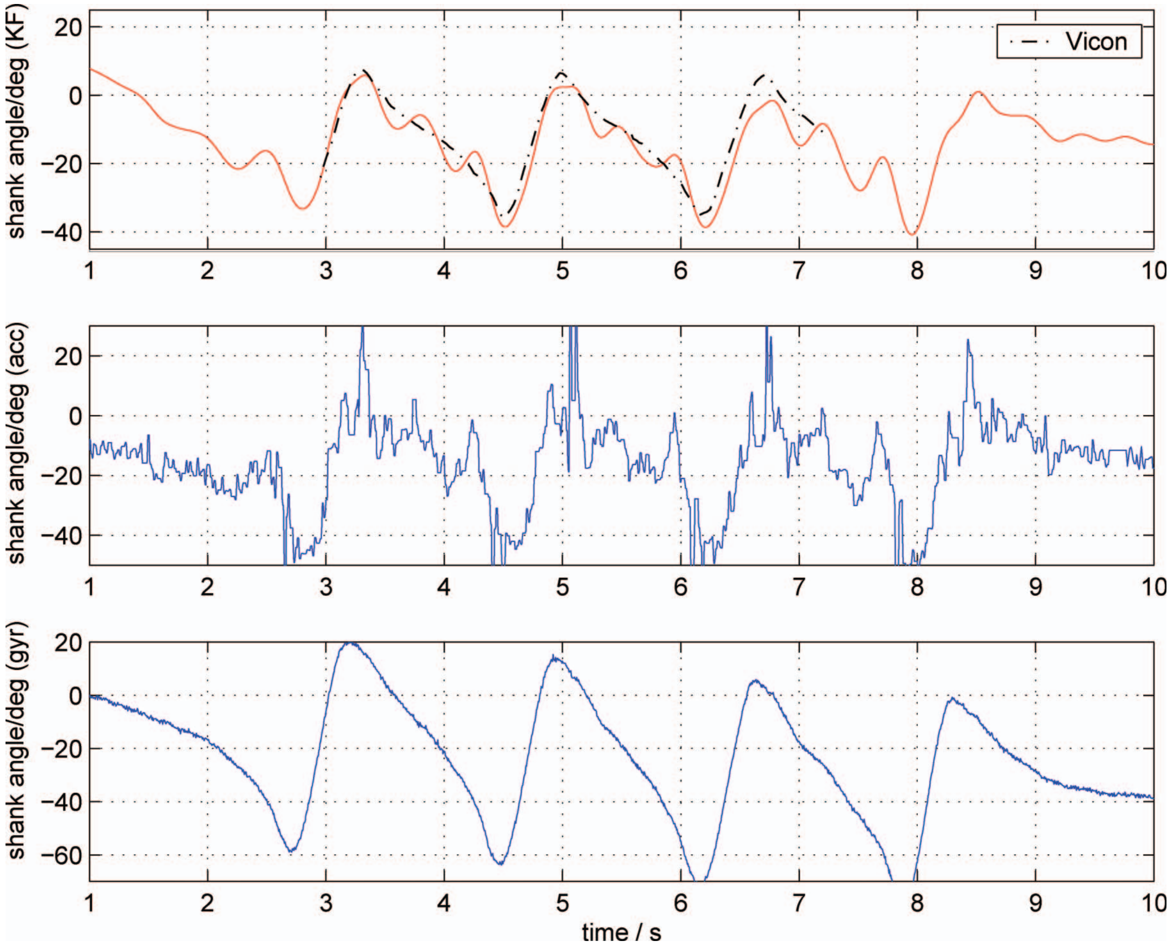

Figure 6. The Kalman filter (KF) is a good solution to overcome gyroscope (gyr) integration error and accelerometer (acc) dynamic restriction.

tests while subject AO walked on the treadmill in order to test the repeatability and reliability of the FES triggering. In this case there was no actual stimulation applied to the walking subject, only the output (trigger) signal was measured. Figure 8 clearly shows that no mistake had occurred during cyclical treadmill walking.

4. Discussion

The proposed method may present a good alternative to existing single sensor methods for tilt estimation for the purpose of swing analysis, where optical motion systems cannot be applied. Several tilt sensors as well as a two-axis accelerometer are based on the low-pass filter [4]. The cut-off frequency of such a filter is very low (approximately 3 Hz). Realization of such a filter may cause difficulties in cases where a steep slope is required, as the filter order may increase enormously, resulting in an inadmissible time delay. The steep slope may be necessary due to the higher frequency response in the heel contact phase. Therefore the use of the accelerometer based single sensor tilt has proved unsuitable for shank ankle estimation where the movement dynamics of the extremities requires a wider frequency range. One of the possible solutions has been presented in this paper. The implementation of a gyroscope as the main source of sensory information for the angle estimation algorithm, using a Kalman filter and accelerometer data could be a good solution.

Analysis of the proposed method convinced us that the system matrix was time-invariant. Consequently, formulation of the Kalman filter equations was introduced to simplify the process. Thus the Kalman gain had to be computed only once and remained constant. Considering the equations in detail we came to the conclusion that the outcome was more convenient for real-time use than we had expected. The proposed indirect Kalman filter, in fact, became a second order complementary filter with two inputs. Filter analysis

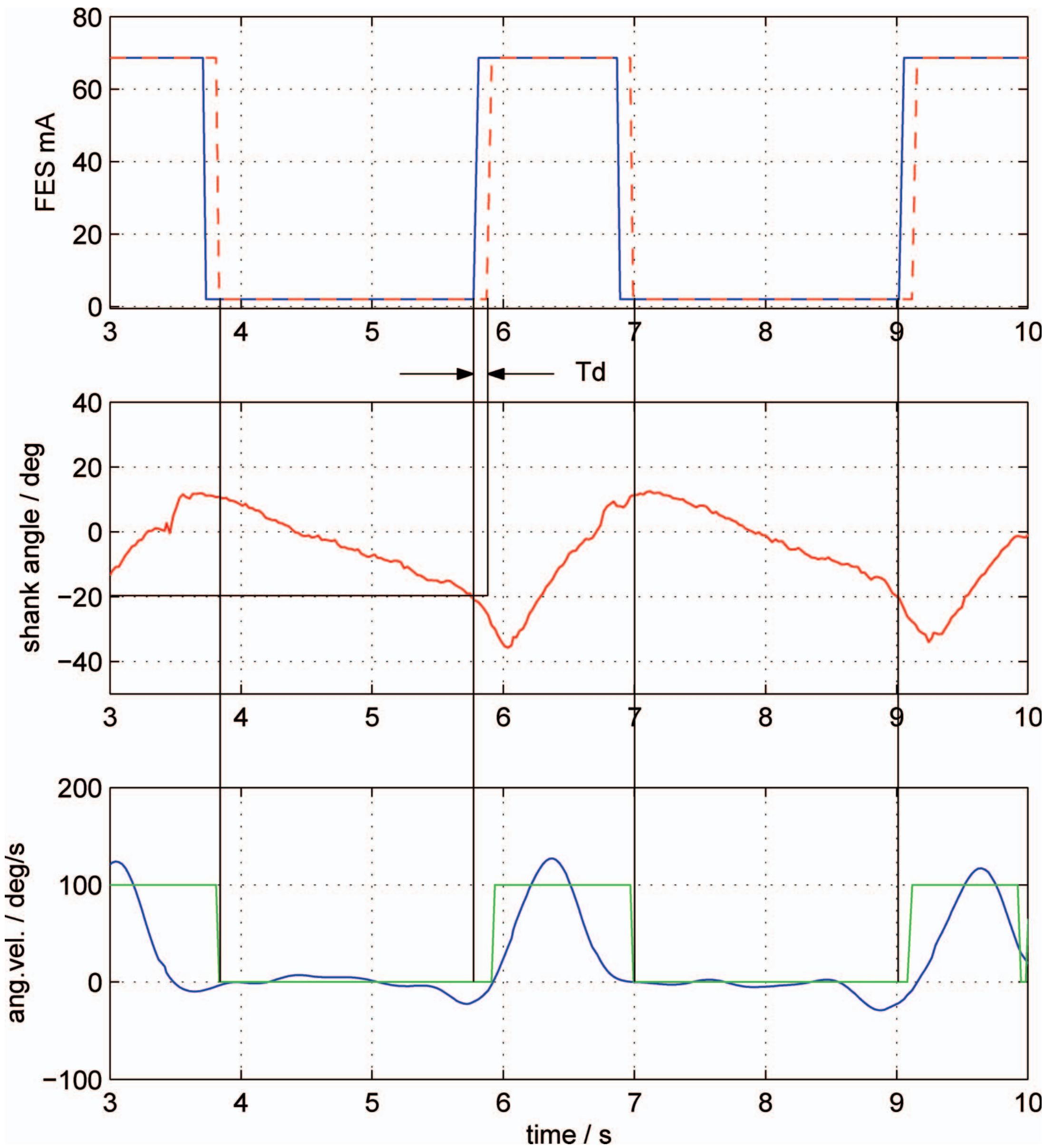

Figure 7. Shank angle was used to trigger functional electrical stimulation. When the subject proceeded to the terminal stance and the shank angle reached 20° inclination, the stimulation had started considering the pre-set time delay T_d. When the swing phase (shown on the graph below) ended, the electrical stimulation was terminated.

showed that an alternative to the proposed method could have been realized as an algorithm with two separately designed filters, a low-pass for accelerometer based tilt sensor filter and high-pass filter for the integrated shank angular velocity. The problem that arises here is related to the selection of the appropriate cut-off frequency. The latter could have been determined by optimization methods that are based on minimization of the signal error when reiteratively changing the coefficients of the low and high pass digital filters [16] to achieve the optimal cut-off frequency.

The measurements were based on healthy subjects walking, in order to evaluate the measurement system in an evaluation process that is ethically incontestable, releasing us from submitting a solicitation to the Ethical Committee. Mention has already been made of the implementation of the sensory system (figure 1) and the algorithm in the FES gait re-education system, which was tested and applied to an incomplete spinal cord injured patient during the treadmill rehabilitation process [7].

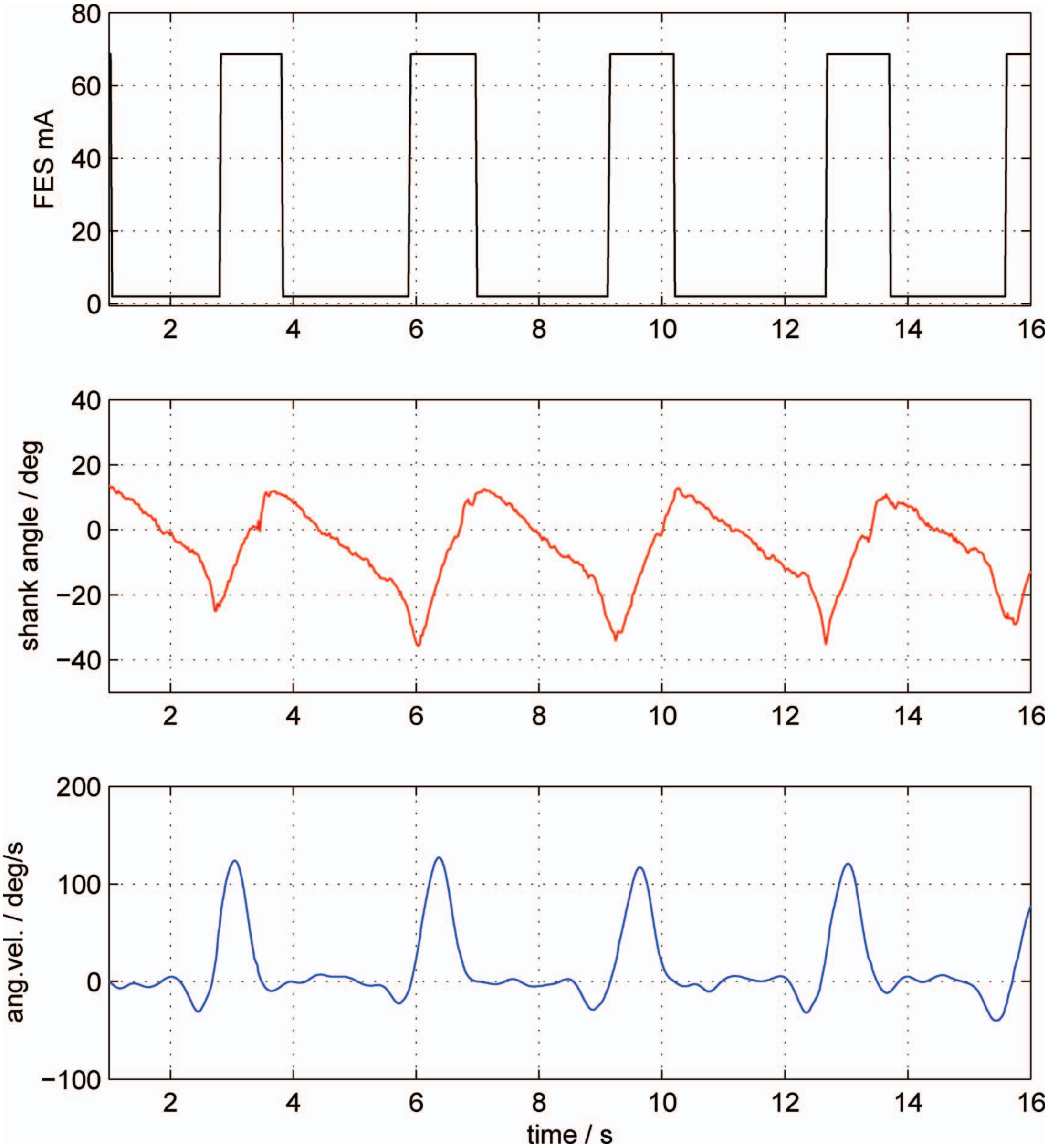

Figure 8. Shank estimation and simulated FES triggering during healthy person (AO) walking on the treadmill. The figure shows that in the terminal stance, when FES triggering takes place, the method is not dubious.

5. Conclusion

The described method of shank angle estimation was demonstrated to be reliable and efficient for FES triggering with no resulting difficulties. The instant of triggering was in compliance with the starting moment of the lower extremity forward swing.

Our work with patients has shown that wearing a lot of equipment is unpopular. Optical position measurement systems or camera based systems are not appropriate alternatives for most rehabilitation centres. Most do not have the necessary equipment, or it may be located in the kinesiologic laboratory, which is usually far from the clinical environment. Our reasonably small device, containing two sensor groups, has proved successful. Therefore the use of mathematical algorithms may be a very convenient solution for obtaining desired values that have not been directly measured.

Acknowledgments

The authors wish to acknowledge the financial support of the Republic of Slovenia Ministry of Education, Science and Sport and Japanese Society for Promotion of Science

(JSPS). Special thanks also to Prof. Ryoko Futami and Andrej Olenšek.

References

[1] Bajd, T., Kralj, A., Štefančič, M. and Lavrač, N., 1999, Use of functional electrical stimulation in the lower extremities of incomplete spinal cord injured patients. *Artificial Organs*, **23,** 403 – 409.

[2] Kralj, A. and Bajd, T., 1989, *Functional electrical stimulation: standing and walking after spinal cord injury* (Boca Raton, FL: CRC Press, 1989).

[3] Willemsen, A.T.H.M., Bloemhof, F. and Boom, H.B.K., 1990, Automatic stance-swing phase detection from accelerometer data for peroneal nerve stimulation. *IEEE Transactions on Biomedical Engineering*, **37,** 1201 – 1208.

[4] Dai, R., Stein, R.B., Andrews, B.J., James, K.B. and Wieler, M., 1996, Application of tilt sensors in functional electrical stimulation. *IEEE Transactions on Rehabilitation Engineering*, **4,** 63 – 72.

[5] Barbeau, H., Ladouceur, M., Mirbagheri, M.M. and Kearney, R.E., 2002, The effect of locomotor training combined with functional electrical stimulation in chronic spinal cord injured subjects: walking and reflex studies. *Brain Research Reviews*, **40,** 274 – 291.

[6] Bajd, T., Cikajlo, I., Šavrin, R., Erzin, R. and Gider, F., 2000, FES rehabilitative systems for re-education of walking in incomplete spinal cord injured persons. *Neuromodulation*, **3,** 167 – 174.

[7] Cikajlo, I., Matjačič, Z. and Bajd, T., 2003, Development of gait re-education system in incomplete spinal cord injury. *Journal of Rehabilitation Medicine*, **35,** 213 – 216.

[8] Cikajlo, I. and Bajd, T., 2003, FES gait re-education: The swing phase estimation. *Neuromodulation*, **6,** 122 – 127.

[9] Cikajlo, I. and Bajd, T., 2002, Swing phase estimation in paralyzed persons walking. *Technology & Health Care*, **10,** 425 – 433.

[10] Tong, K. and Granat, M.H., 1999. A practical gait analysis system using gyroscopes. *Medical Engineering & Physics*, **21,** 87 – 94.

[11] Cikajlo, I. and Bajd, T., 2001, Use of artificial sensors in FES gait reeducation system. In R.J. Triolo (Ed.) *6th Annual Conference of the International Functional Electrical Stimulation Society*, 16–20 June 2001, Cleveland, OH, USA, pp. 135 – 137.

[12] Farrenkopf, R., 1978, Analytic steady-state accuracy solutions for two common spacecraft estimators. *Journal of Guidance and Control*, **1,** 282 – 284.

[13] Kalman, R.E., 1960, A new approach to linear filtering and prediction problems. *IEEE Transactions of the ASME Journal of Basic Engineering*, **82,** 35 – 42.

[14] Brown, R.G. and Hwang, P.Y.C., 1992, *Introduction to Random Signals and Applied Kalman Filtering*, Second edn (New York, USA: John Wiley & Sons).

[15] Kamen, E.W., 1999, *Introduction to optimal estimation* (London: Springer).

[16] Hagiwara, T., Ohba, S., Futami, R. and Hoshimiya, N., 2003, The practical method of posture measurements for lower limb FES control. Technical report, Tohoku University, ECEI, Sendai, Japan, November 2003.

[17] Perry, J., 1992, *Gait analysis: normal and pathological function* (Thorofare: SLACK Incorporated).